Islet Cholesterol Accumulation Due to Loss of ABCA1 Leads to Impaired Exocytosis of Insulin Granules

Janine K. Kruit,[1] Nadeeja Wijesekara,[1] Jocelyn E. Manning Fox,[2] Xiao-Qing Dai,[2] Liam R. Brunham,[1] Gavin J. Searle,[2] Garry P. Morgan,[3] Adam J. Costin,[3] Renmei Tang,[1] Alpana Bhattacharjee,[1] James D. Johnson,[4] Peter E. Light,[2] Brad J. Marsh,[3] Patrick E. MacDonald,[2] C. Bruce Verchere,[5] and Michael R. Hayden[1]

OBJECTIVE—The ATP-binding cassette transporter A1 (ABCA1) is essential for normal insulin secretion from β-cells. The aim of this study was to elucidate the mechanisms underlying the impaired insulin secretion in islets lacking β-cell ABCA1.

RESEARCH DESIGN AND METHODS—Calcium imaging, patch clamp, and membrane capacitance were used to assess the effect of ABCA1 deficiency on calcium flux, ion channel function, and exocytosis in islet cells. Electron microscopy was used to analyze β-cell ultrastructure. The quantity and distribution of proteins involved in insulin-granule exocytosis were also investigated.

RESULTS—We show that a lack of β-cell *ABCA1* results in impaired depolarization-induced exocytotic fusion of insulin granules. We observed disturbances in membrane microdomain organization and Golgi and insulin granule morphology in β-cells as well as elevated fasting plasma proinsulin levels in mice in the absence of β-cell *ABCA1*. Acute cholesterol depletion rescued the exocytotic defect in β-cells lacking *ABCA1*, indicating that elevated islet cholesterol accumulation directly impairs granule fusion and insulin secretion.

CONCLUSIONS—Our data highlight a crucial role of ABCA1 and cellular cholesterol in β-cells that is necessary for regulated insulin granule fusion events. These data suggest that abnormalities of cholesterol metabolism may contribute to the impaired β-cell function in diabetes. ***Diabetes*** **60:3186–3196, 2011**

Why β-cells fail in type 2 diabetes is a question of intense interest. Abnormalities in islet cholesterol metabolism have recently emerged as a potential contributor to β-cell dysfunction (1). Type 2 diabetes frequently co-occurs with abnormalities of plasma lipoproteins, and "diabetic dyslipidemia" is characterized by low levels of HDL cholesterol and elevated triglycerides (2). Low HDL cholesterol is a risk factor for the development of type 2 diabetes (3) and is inversely correlated with β-cell function in patients with type 2 diabetes (4), suggesting that abnormalities of plasma lipids may affect the pathogenesis of this disease. Elevated plasma cholesterol levels induce islet cholesterol accumulation in mice (5–7), and exposure of β-cells to high levels of cholesterol causes dysfunction and death (6–8). In mice fed a high-fat diet, accumulation of cholesterol in islets was recently shown to discriminate between mice that do and do not develop diabetes (9). Conversely, infusion of HDL cholesterol in humans improves β-cell function (10). Together, these data provide compelling evidence that cholesterol metabolism plays an important and previously unrecognized role in β-cell function.

We identified ATP-binding cassette transporter A1 (ABCA1) as a key molecule in islet cholesterol metabolism (5). ABCA1 mediates the rate-limiting step in HDL biogenesis in humans: the efflux of cellular cholesterol and phospholipids. In mice, the targeted deletion of *ABCA1* in β-cells leads to islet cholesterol accumulation, impaired nutrient-stimulated insulin secretion, and markedly impaired glucose tolerance (5). Moreover, humans heterozygous for mutations in *ABCA1* have impaired β-cell function (11). Models of ABCA1 deficiency offer a unique opportunity to understand the role of cholesterol metabolism in diabetes. The specific mechanisms by which ABCA1 and islet cholesterol metabolism influence β-cell function are unknown. In this study, we show that ABCA1 deficiency in β-cells leads to reduced insulin granule exocytosis, altered microdomain organization and Golgi ultrastructure, and impaired proinsulin processing.

RESEARCH DESIGN AND METHODS

Animals. *ABCA1* β-cell–specific knockout and control *ABCA1* floxed mice have been described previously (5). Mice were bred to a pure C57Bl6 background as described previously (12). All studies were approved by the University of British Columbia Animal Care Committee.

Physiologic and metabolic studies. Intraperitoneal glucose tolerance tests, islet isolation, glucose-stimulated insulin secretion, and islet cholesterol measurements were performed as described previously (5,6). Plasma proinsulin levels were measured using the rat/mouse proinsulin ELISA kit (Mercodia, Uppsala, Sweden) (13).

For cholesterol efflux measurements, islets were loaded with 1 μCi/mL [^{3}H] cholesterol overnight. Islets were then washed and incubated in RPMI 1640 medium containing 0.1% BSA, with or without 10 μg/mL human apolipoprotein A-I (apoA-I) (Athens Research and Technology, Athens, GA), for 4 h. Medium was collected, and cells were lysed in 0.1 N NaOH/0.1% SDS. Radioactivity in samples was measured by scintillation counting. Cholesterol efflux is expressed as a percentage of counts in medium over total (medium plus islets) counts.

Ca^{2+} imaging. Islets were dispersed and imaged as described previously (14). Cytosolic Ca^{2+} was imaged in Fura-2-acetoxymethyl–loaded cells. Area under the curve was measured over the first 10 min of 10 mmol/L glucose, the first 5 min of 100 μmol/L tolbutamide, and the first 5 min of 30 mmol/L KCl perfusion. Cells that failed to raise the 340:380 ratio 2 SDs above the baseline within 5 min after treatment with 10 mmol/L glucose were excluded from the analysis.

From the [1]Departments of Medical Genetics, Centre for Molecular Medicine, and Therapeutics, Child and Family Research Institute, University of British Columbia, Vancouver, British Columbia, Canada; the [2]Department of Pharmacology, Alberta Diabetes Institute, University of Alberta, Edmonton, Alberta, Canada; the [3]Institute for Molecular Bioscience, The University of Queensland, Brisbane, Queensland, Australia; the [4]Department of Cellular and Physiological Sciences, University of British Columbia, Vancouver, British Columbia, Canada; and the [5]Departments of Pathology & Laboratory Medicine and Surgery, Child and Family Research Institute, University of British Columbia, Vancouver, British Columbia, Canada.

Corresponding author: Michael R. Hayden, mrh@cmmt.ubc.ca.

Received 25 January 2011 and accepted 2 September 2011.

DOI: 10.2337/db11-0081

This article contains Supplementary Data online at http://diabetes.diabetesjournals.org/lookup/suppl/doi:10.2337/db11-0081/-/DC1.

J.K.K. and N.W. contributed equally to this work.

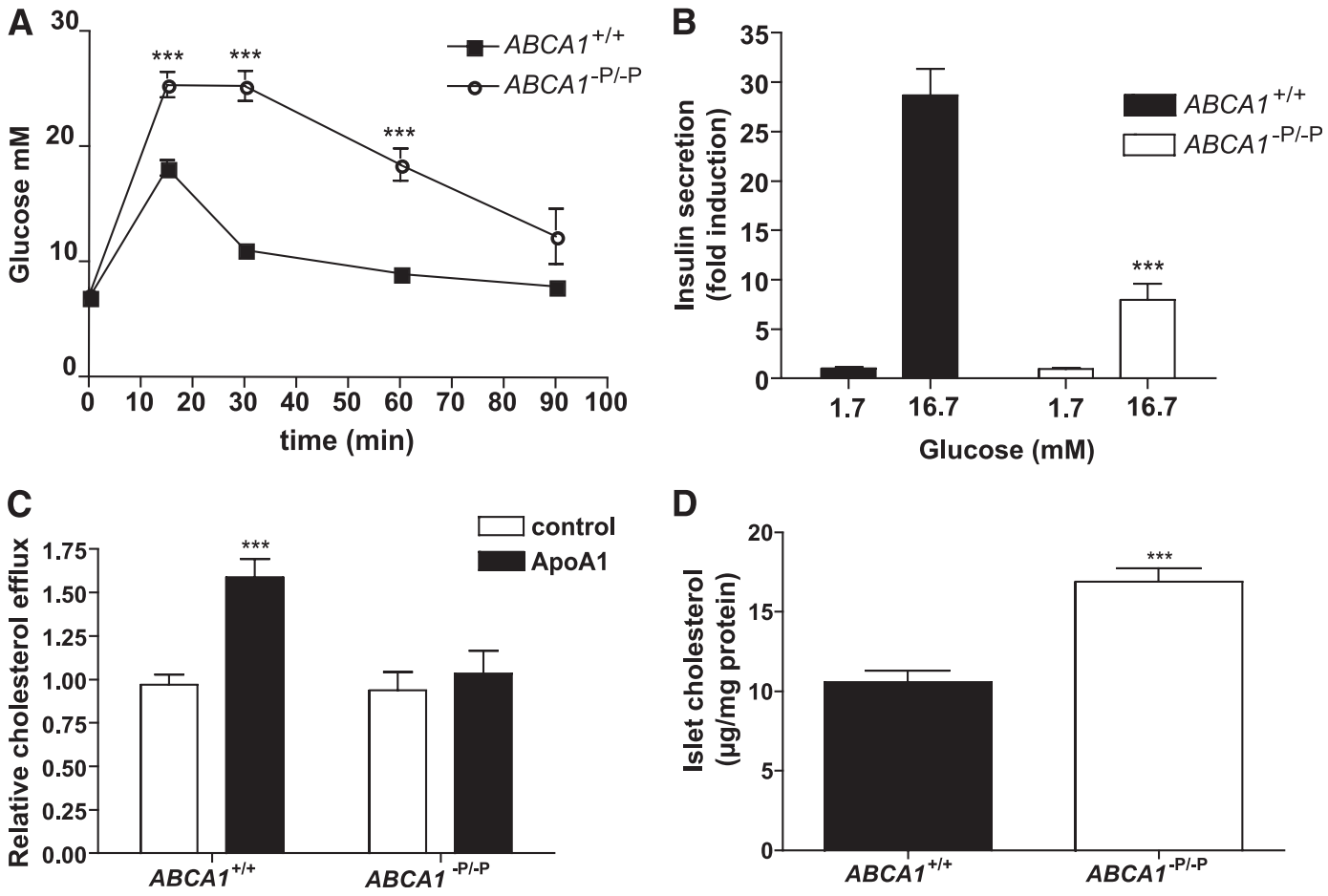

FIG. 1. Mice lacking β-cell *ABCA1* show impaired glucose tolerance, impaired insulin secretion, impaired islet cholesterol efflux, and increased islet cholesterol levels. *A*: Plasma glucose levels during glucose tolerance test ($n = 5$). *B*: Glucose-stimulated insulin secretion from isolated islets. Values represent pooled data from three separate experiments; each consisted of pooled islets from three mice per genotype, and values are expressed as percent of islet content relative to basal secretion, which is arbitrarily set to 1. *C*: Cholesterol efflux toward apoA1. Values represent pooled data from three separate experiments. *D*: Islet cholesterol levels ($n = 4$). ***$P < 0.001$ compared with controls.

Electrophysiology. Ca^{2+} current recordings were made in the whole-cell configuration of the patch-clamp technique from isolated β-cells. Recordings were digitized at 20 KHz and filtered at 5 KHz using the Axopatch200B patch-clamp amplifier and Clampex 8.0 (Molecular Devices Corp., Union City, CA). Bath perfusate contained (in mmol/L): NaCl, 95; CsCl, 5; $MgCl_2$, 0.6; $BaCl_2$, 20; HEPES, 5; glucose, 10; tetraethylammonium-Cl, 20; and 0.0005 tetrodotoxin (pH adjusted to 7.4 with NaOH, 21–24°C).

Patch pipettes were pulled from borosilicate glass (GB150-86-15; Sutter Instrument Co., Novato, CA) to yield resistances between 1.7 and 2.0 MΩ when backfilled with buffer solution. Pipette tips were filled with a buffer solution containing (in mmol/L): CsCl, 120; tetraethylammonium-Cl, 20; $MgCl_2$, 2; EGTA, 10; HEPES, 10; and ATP, 2 (pH adjusted to 7.2 with CsOH).

Cells were voltage-clamped at −80 mV, and whole-cell capacitance was determined from analog compensation. Series resistance compensation of 80–90% was applied. To evoke total whole-cell Ca^{2+} currents, cells were hyperpolarized to −90 mV (200-ms duration) and then depolarized to 10 mV (250-ms duration). Leak subtraction was applied using a p/5 protocol.

K^+ current recordings were performed with an EPC10 patch-clamp amplifier controlled with PatchMaster software (HEKA Electronik, Lambrecht, Germany) as described previously (15). Data were analyzed using FitMaster (HEKA Electronik) and SigmaPlot 10 software (Systat Software, Inc., Point Richmond, CA).

Capacitance measurements were performed as described previously (16). Whole-cell capacitance responses were normalized to initial cell size and expressed as femtofarad per picofarad.

FM1-43 imaging. Islet cells were dispersed and plated on glass coverslips. Cells were loaded with 8 μmol/L FM1-43 in voltage-dependent K^+ (K_v) bath solution (as described above) for 10 min at 37°C. Cells were then imaged on an upright epifluorescence microscope (Olympus Canada, Inc., Markham, ON, Canada) at original magnification ×10. Fluorescence emission was measured at 520 nm after excitation at 480 nm at a rate of 0.33 frames/min. Cells were bathed in K_v bath solution at 37°C, and 1 mol/L KCl was added to adjust the final concentration of KCl to 25 mmol/L as indicated.

Electron microscopy. Islets were cultured in Hams' F-10 medium containing 10% (v/v) FBS and 6 mmol/L D-glucose and high-pressure frozen, freeze substituted, processed, and plastic embedded, essentially as described previously (17). Ribbons of thin (40–60-nm) sections were cut on a microtome for survey at 80–100 keV to assess the quality of islet freeze preservation on Tecnai T12 (FEI Company, Hillsboro, OR) or JEOL 1011 (JEOL Australia, Frenchs Forest, NSW, Australia) microscopes.

Stereology. Sample grids were viewed on the electron microscope at appropriate magnification and digital images captured at random to ensure an unbiased analysis/quantification. After capturing or freezing each image (or in live mode), an appropriate imaging grid (e.g., 1,000 × 1,000 nm) stored as a macro program in the camera/image analysis software was overlaid onto the image field. Points at which the grid lines intersected were counted for the cytoplasm versus other organelles compartments such as mitochondria, digestive/autophagic structures, and mature insulin granules. The relative volume of a given compartment in the cell was calculated by measuring the ratio of points over the compartment of interest/points over the cytoplasm, expressed as a percentage of cytoplasmic volume occupied by that compartment.

Lipid raft isolation and Western blotting. MIN6 cells were lysed in 170 μL ice-cold 2-(*N*-morpholino)ethanesulfonic acid (Mes)-buffered saline (25 mmol/L Mes, 150 mmol/L NaCl, pH 6.5) containing 0.25% Triton X-100 and protease inhibitor mix and incubated at 4°C for 30 min. The lysate was homogenized with 20 strokes of a Dounce homogenizer. Equal amounts of protein in 150 μL were added to an equal volume of 80% (w/v) sucrose and overlayed with 300 μL of 30% sucrose and 225 μL of 5% sucrose. After centrifugation at 54,000 rpm in a Beckman TLS-55 rotor (Beckman Coulter, Inc., Fullerton, CA) for 20 h, 70-μL fractions were collected from the top of the gradient and designated fractions number 1 (top) through 11 (bottom).

For epidermal growth factor (EGF) signaling, islets were incubated in RPMI 1640 medium with 0.5% BSA overnight, stimulated with 50 ng/mL EGF for 20 min, and lysed in SDP+ buffer (50 mM Tris pH 8.0, 150 mM NaCl, 1% Igepal, 40 mM B-glycerophosphate, 10 mM NaF, 1× Roche complete protease inhibitor, 1 mM sodium orthovanadate, and 800 μM PMSF) after washing.

Equivalent amounts of total protein (30 μg) or equal volumes (lipid rafts) were immunoblotted as previously described (6) using antibodies to flotillin (BD Transduction Laboratories, Mississauga, ON, Canada), synaptosomal-associated protein-25 (Covance, Princeton, NJ), transferrin receptor (Invitrogen, Burlington, ON, Canada), AKT and pAKT (Ser-473; Cell Signaling, Beverly, MA), vesicle-associated membrane protein 2 (VAMP-2), syntaxin-4, syntaxin-1, and actin (Abcam, Cambridge, MA). Protein bands were analyzed by densitometry using Quantity One (Bio-Rad, Hercules, CA) or ImageJ software (National Institutes of Health, Bethesda, MD).

Statistical analysis. Data are presented as means ± SE. Differences between groups were calculated by the Student *t* test for two groups or one-way ANOVA with the Newman-Keuls post-test for three groups, with $P = 0.05$ considered significant.

RESULTS

Defective insulin secretion in mice lacking β-cell *ABCA1* is independent of background strain. Previous studies of mice with β-cell deletion of *ABCA1* (*ABCA1*$^{-P/-P}$ mice) were performed on a mixed C57Bl6/129SvEV background (5). Because background strain may influence glucose metabolism and insulin secretion (18), we first confirmed that the insulin secretory defect in mice carrying the *ABCA1*-null mutation was maintained on a pure C57Bl6 background. Lack of β-cell *ABCA1* in C57Bl6 mice resulted in impaired glucose tolerance (Fig. 1*A*) and insulin secretion (Fig. 1*B*) at age 4 months, consistent with previous data on a mixed background (5). Islets lacking β-cell *ABCA1* also had impaired cholesterol efflux toward apoA1 (Fig. 1*C*). In addition, islets isolated from *ABCA1*$^{-P/-P}$ mice had increased cholesterol levels (Fig. 1*D*). These data indicate that the phenotype observed in mice lacking β-cell *ABCA1* on a mixed background persists on a pure C57Bl6 background strain.

Lack of *ABCA1* results in decreased depolarization-evoked $[Ca^{2+}]_i$ influx with normal voltage-dependent Ca^{2+} channel activity. Glucose stimulates insulin secretion by inducting electrical activity, Ca^{2+} influx, and subsequent Ca^{2+}-dependent exocytosis of insulin-containing granules (19). Studies show that cholesterol loading of cultured β-cells results in decreased glucose-stimulated Ca^{2+} influx (7,20). To determine whether cholesterol accumulation due to lack of *ABCA1* in β-cells influences Ca^{2+} influx, we measured intracellular calcium ($[Ca^{2+}]_i$) levels by Fura-2 acetoxymethyl imaging in single β-cells. At 3 mmol/L glucose, we noted a modest increase in basal $[Ca^{2+}]_i$ in *ABCA1*-deficient β-cells (Table 1). The shapes of the glucose-stimulated $[Ca^{2+}]_i$ increases were qualitatively similar in β-cells from control and *ABCA1*$^{-P/-P}$ mice (Fig. 2*A*). Total $[Ca^{2+}]_i$ was modestly decreased in β-cells lacking *ABCA1* upon stimulation with 10 mmol/L glucose or depolarization with KCl or tolbutamide, the K_{ATP} channel inhibitor (Table 1), indicating that the calcium influx defect arises from perturbations downstream of glucose sensing and metabolic pathways.

At the plasma membrane, Ca^{2+} influx via voltage-dependent Ca^{2+} channels (VDCCs) is the major trigger for insulin granule exocytosis (21). A recent report suggested that cholesterol enrichment induced a decrease in VDCC-mediated extracellular Ca^{2+} influx in isolated β-cells (20). Therefore, we measured calcium current density by whole-cell patch clamp studies but observed no difference in the magnitude of currents between control and *ABCA1*-deficient β-cells (Fig. 2*B* and *C*). Furthermore, the activity of K_v channels, which has been implicated in the repolarization of β-cell membrane potential leading to the closure of VDCCs and has been shown to be sensitive to changes in cholesterol levels (20,22), was similar between control and *ABCA1*-deficient β-cells (Fig. 2*D* and *E*). Although the modest changes in depolarization-evoked $[Ca^{2+}]_i$ could lead to some reduction in insulin secretion, the lack of significant change in VDCC and K_v channel activity suggests the existence of additional defects downstream of Ca^{2+} influx that contribute to the impaired insulin secretion in β-cells lacking *ABCA1*.

***ABCA1* deficiency leads to defective exocytosis in β-cells.** To investigate whether a distal exocytotic defect may be present in β-cells lacking *ABCA1*, we performed FM1-43 destaining and whole-cell membrane capacitance measurements. Both methods quantify the plasma membrane surface area, which transiently increases each time a granule undergoes exocytosis and is incorporated into the membrane. A stepwise membrane depolarization from −70 to 0 mV activates VDCCs and thereby triggers the exocytotic fusion of secretory vesicles with the plasma membrane. Depolarization of the membrane led to similar Ca^{2+} currents in control and *ABCA1*-null β-cells (Fig. 3*A*). Whereas depolarization led to increased capacitance in control β-cells, this effect was markedly impaired in β-cells lacking *ABCA1* (Fig. 3*B*). Furthermore, KCl-induced exocytosis (as measured by FM1-43 destaining) was profoundly reduced in *ABCA1*-null β-cells (Fig. 3*C*). FM1-43 has been extensively used for monitoring insulin granule exocytosis (23–25), although it should be noted that FM1-43 may

TABLE 1
Quantification of calcium imaging of dispersed β-cells isolated from control and *ABCA1*$^{-P/-P}$ mice

Variable	*ABCA1*$^{+/+}$	*n*	*ABCA1*$^{-P/-P}$	*n*	*P*
Basal $[Ca^{2+}]_i$ ratio	0.343 ± 0.004	18	0.368 ± 0.006	17	0.0002
Response to					
Glucose (10 mmol/L)					
Peak ratio	1.324 ± 0.044	10	1.258 ± 0.017	9	0.197
Area under the curve	3.542 ± 0.212	10	2.916 ± 0.135	9	0.027
Tolbutamide (100 μmol/L)					
Peak ratio	1.313 ± 0.036	5	1.183 ± 0.055	4	0.078
Area under the curve	2.621 ± 0.126	5	2.213 ± 0.093	4	0.042
KCl (30 mmol/L)					
Peak ratio	1.528 ± 0.059	10	1.400 ± 0.047	10	0.105
Area under the curve	3.943 ± 0.136	10	3.429 ± 0.162	10	0.024

Data are presented as mean ± SE.

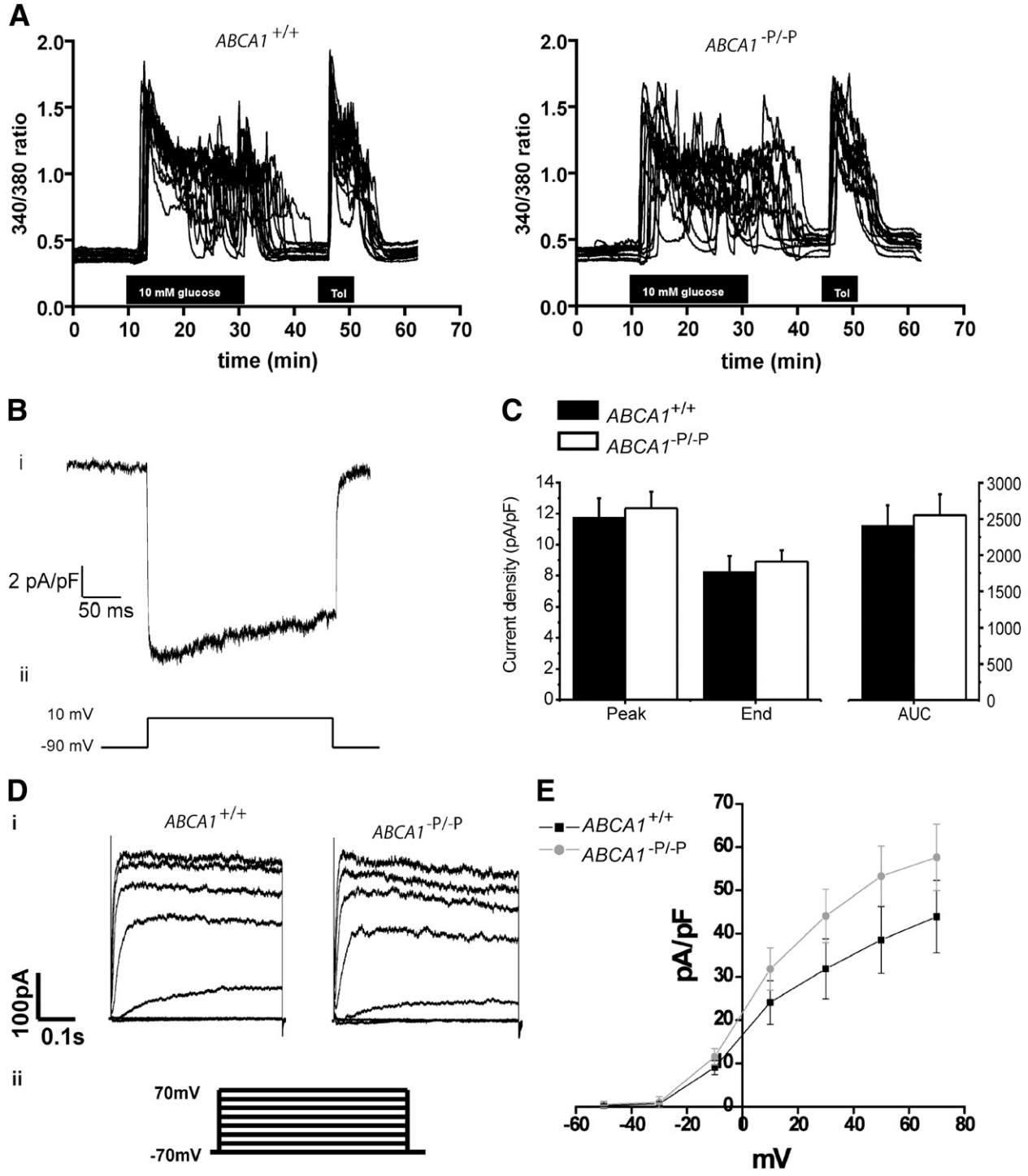

FIG. 2. Ca^{2+} influx and ion channel activity unaltered in β-cells lacking *ABCA1*. *A*: Influence of 10 mmol/L glucose and 100 μmol/L tolbutamide (Tol) on $[Ca^{2+}]_i$. $[Ca^{2+}]_i$ was monitored as the 340:380 nm fluorescence ratio. Representative traces of individual β-cells are shown. *B*: Ca^{2+} current density from β-cells: *i*) representative current density recording and *ii*) voltage clamp protocol used to elicit Ca^{2+} currents. *C*: Group data for control (n = 14) and $ABCA1^{-P/-P}$ (n = 11) mice for peak current density, mean current density measured during the last 10 ms of the depolarization step (End), and total Ca^{2+} current density for entire depolarization step measured as area under the curve (AUC). *D*: K^+ current density from β-cells: *i*) representative current density recording and *ii*) voltage clamp protocol used to elicit K^+ currents. *E*: Group data for control (n = 8) and $ABCA^{-P/-P}$ mice (n = 7) during different voltages.

also label synaptic-like microvesicles, which also undergo Ca^{2+}-dependent exocytosis (26). Nonetheless, these data suggest an exocytotic defect in *ABCA1*-deficient β-cells that probably contributes to impaired insulin secretion.

To determine whether *ABCA1* deficiency might uncouple VDCC activity from insulin granule exocytosis, we measured capacitance during prolonged membrane depolarization, causing a more global Ca^{2+} increase and a reduction in the requirement for direct VDCC-granule coupling. The change in capacitance of *ABCA1*-deficient β-cells during prolonged depolarization was severely blunted (Fig. 3*D* and *E*). These data indicate that β-cells lacking *ABCA1* fail to translate the

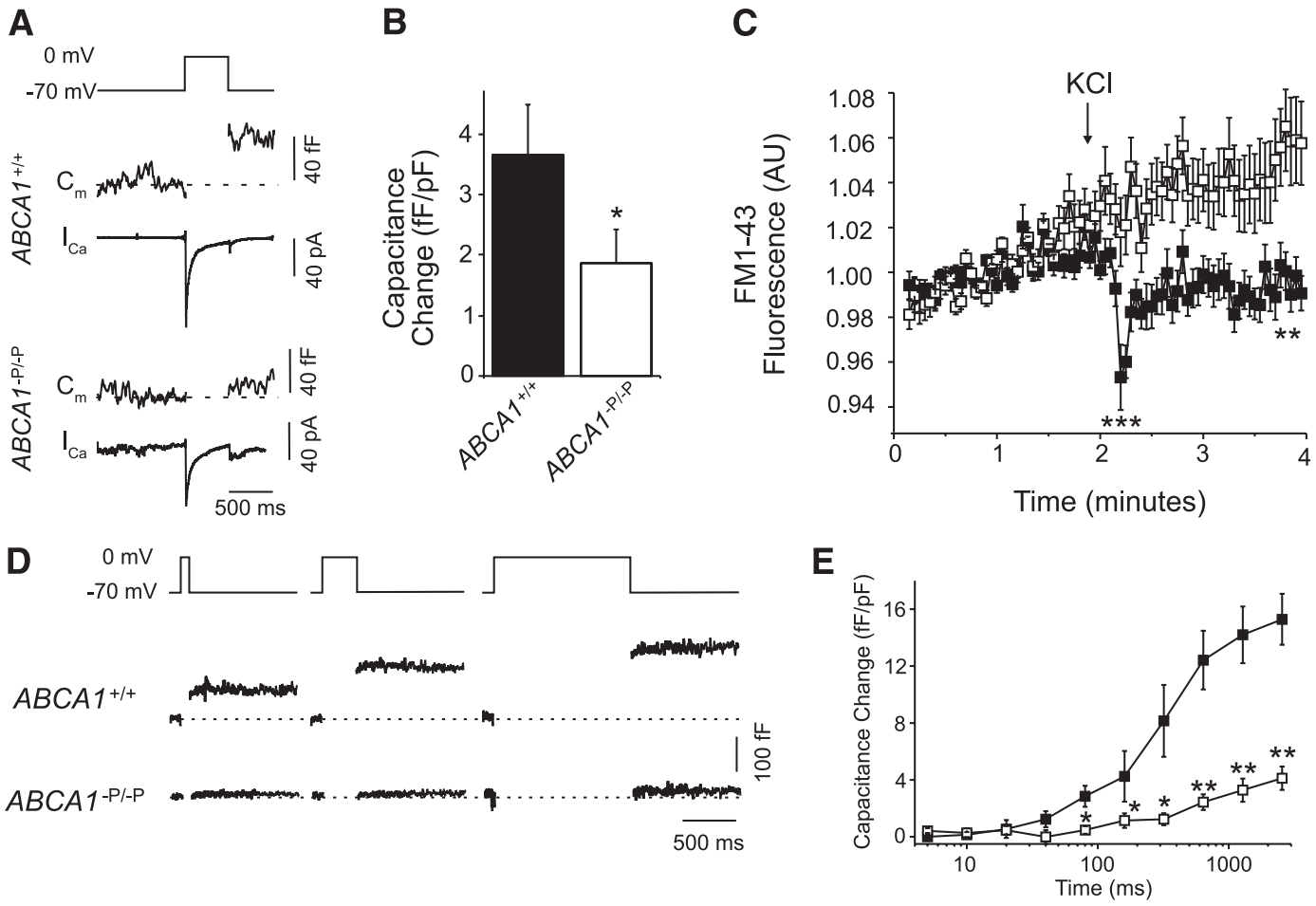

FIG. 3. Depolarization-induced exocytosis is impaired in β-cells lacking *ABCA1*. *A*: β-Cell membrane capacitance (C_m) and voltage-dependent Ca^{2+} currents (I_{Ca}) in response to a single 500-ms depolarization. *B*: The average exocytotic response, normalized to initial cell size (n = 40–58). *C*: FM1-43 destaining in response to 30 mmol/L KCl in *ABCA1*$^{+/+}$ (n = 23, ■) and *ABCA1*$^{-P/-P}$ (n = 24, □) β-cells. AU, arbitrary unit. *D*: Capacitance measurements after a series of membrane depolarizations of progressively increasing duration. *E*: The average responses of *ABCA1*$^{+/+}$ (n = 40, ■) and *ABCA1*$^{-P/-P}$ (n = 58, □) β-cells. *P < 0.05, **P < 0.01, and ***P < 0.001 compared with controls.

chemical signal of elevated cellular calcium into exocytotic events. These data also suggest that defective granule exocytosis in β-cells lacking *ABCA1* is downstream of Ca^{2+} entry into the β-cell.

Altered Golgi ultrastructure and impaired proinsulin processing in β-cells of *ABCA1*$^{-P/-P}$ mice. Defective granule exocytosis after Ca^{2+} entry could result from a paucity of secretory granules available at the plasma membrane, impaired granule assembly or transport, or alterations in the exocytotic machinery at the plasma membrane. To investigate the possibility of reduced availability of insulin-containing granules, we performed detailed quantitative electron microscopic analysis of β-cells in islets isolated from *ABCA1*$^{-P/-P}$ and control mice. We observed no significant differences in the cytoplasmic density of mature insulin granules (Supplementary Table 1) or the number of insulin granules close (<100 nm) to the plasma membrane between β-cells from *ABCA1*$^{-P/-P}$ and control mice (Fig. 4*A* and *B*). Availability of granules at the plasma membrane is therefore unlikely to explain the secretory defect in *ABCA1*-deficient islets.

Although the number of insulin granules was preserved, the ultrastructure of mature insulin granules in β-cells of mice lacking *ABCA1* was more heterogeneous with respect to mean diameter (Supplementary Fig. 1*A* and *B*), indicating that mechanisms that regulate insulin granule biogenesis at the Golgi are disrupted by lack of β-cell *ABCA1*. Indeed, Golgi cisternae from *ABCA1*-deficient β-cells (Fig. 5*C* and *D*) appeared more tightly stacked and demonstrated increased lateral continuity resulting in a more ordered architecture of the Golgi ribbon compared with those of control β-cells (Fig. 5*A* and *B*). Moreover, there was an increased tendency of regions of the Golgi ribbon to form circular organization in β-cells lacking *ABCA1*. Circular Golgi organization has previously been reported in kidney cells in which protein exit and membrane traffic out of the Golgi was blocked by incubation at 20°C (27). Collectively, these observations indicate that islet cholesterol accumulation accompanying loss of *ABCA1* leads to fundamental alterations of Golgi structure that would be expected to impair membrane trafficking and carrier formation and contribute to impaired exocytosis of insulin granules. Consistent with this, *ABCA1*$^{-P/-P}$ mice showed increased plasma proinsulin levels after fasting compared with *ABCA1*$^{+/+}$ mice (8.61 ± 0.95 vs. 4.26 ± 1.79 pmol/L, P = 0.03), but plasma insulin levels were unaltered (5).

Lack of *ABCA1* disrupts membrane domain organization. To investigate whether insulin granule fusion at the plasma membrane is also affected by the absence of *ABCA1*, we

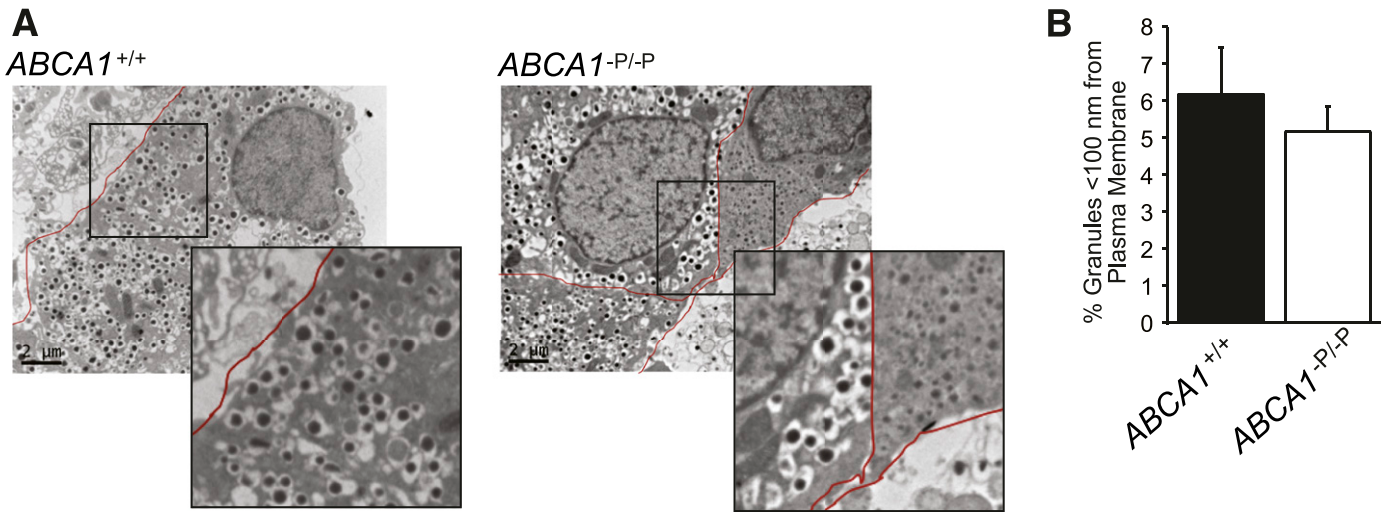

FIG. 4. β-Cells lacking *ABCA1* show similar number of docked granules. *A*: Representative electron micrographs. Insert shows docked granules at the plasma membrane in more detail. *B*: The percentage of secretory granules localized to the plasma membrane (<100 nm) within *ABCA1*$^{+/+}$ and *ABCA1*$^{-P/-P}$ β-cells (n = 13–19). (A high-quality color representation of this figure is available in the online issue.)

next examined the expression of several SNARE (soluble *N*-ethylmaleimide-sensitive factor attachment protein receptor) proteins in islets isolated from control and *ABCA1*$^{-P/-P}$ mice. At the plasma membrane, insulin granules fuse to the plasma membrane by the pairing of SNARE proteins located on the granules and the plasma membrane (28). Protein levels of the major SNARE proteins—SNAP-25, VAMP-2, syntaxin-1, and syntaxin-4—were not significantly altered in islets isolated from *ABCA1*$^{-P/-P}$ mice compared with control mice (Fig. 6*A*).

SNARE proteins are concentrated in cholesterol-dependent microdomains that have functional importance for exocytosis (22,29). Redistribution of SNARE proteins by depletion of membrane cholesterol has been shown to inhibit exocytosis and dopamine release from neuroendocrine cells, and conversely, is associated with elevated exocytic events and insulin secretion from HIT-T15 β-cells (22,30). To examine whether elevated levels of cholesterol could modulate SNAP-25 distribution in β-cells, MIN6 β-cells were loaded with cholesterol, which increased the localization of SNAP-25 into lipid raft fractions. Subsequent cholesterol depletion with methyl-β-cyclodextrin (MβCD) led to the redistribution of SNAP-25 out of the lipid raft fractions (Fig. 6*B*). Flotillin, a well-established marker of lipid rafts, followed a similar pattern after cholesterol loading and depletion, suggesting that these changes are not unique to proteins regulating exocytosis.

EGF signaling, which is sensitive to changes in cholesterol-enriched microdomains (31,32), was measured to confirm changes in microdomain organization in β-cells lacking *ABCA1*. Beside their role in membrane trafficking, cholesterol-enriched microdomains are thought to be of particular importance for signal transduction (33–35). EGF-induced AKT phosphorylation was impaired in islets isolated from *ABCA1*$^{-P/-P}$ mice (Fig. 6*C*). These data suggest that microdomain organization is altered in *ABCA1*-deficient β-cells, which would be expected to interfere with granule exocytosis.

Cholesterol depletion rescues exocytotic defect in β-cells lacking *ABCA1*. To determine whether elevated cellular cholesterol levels associated with *ABCA1* deficiency are causally related to impaired exocytosis, we superfused cells directly with a low concentration of MβCD (10 μmol/L) to deplete cellular cholesterol before and during capacitance measurements (Fig. 7*A*). Change in capacitance in response to pipette dialysis of 200 nmol/L–free Ca^{2+} was markedly blunted in *ABCA1*-deficient β-cells (Fig. 7*B* and *C*). Notably, the exocytotic defect was completely rescued by co-infusion of MβCD. Likewise, the exocytotic response to sequential ten 500-ms depolarizations, which was blunted in the *ABCA1*-null β-cells, was entirely rescued by an acute (2-min) infusion of MβCD before the recording (Fig. 7*D* and *E*). These findings indicate that acute depletion of cellular cholesterol rescues granule exocytosis and suggests that cholesterol accumulation itself, perhaps at or near the site of granule exocytosis, is responsible for the impaired exocytosis and insulin secretion in *ABCA1*-deficient β-cells.

DISCUSSION

Here we show that lack of *ABCA1* in β-cells disrupts insulin granule exocytosis and thereby leads to defective insulin secretion and abnormal glucose homeostasis. Depletion of intracellular cholesterol acutely rescued the exocytotic defect in *ABCA1*-deficient β-cells, showing that cholesterol accumulation is the major factor influencing impaired insulin secretion in β-cells lacking *ABCA1*. Importantly, the finding that cholesterol depletion rescues the exocytotic defect in *ABCA1*-deficient β-cells establishes elevated islet cholesterol as a common mechanism for the impaired insulin secretion that has been observed in numerous animal models that display elevated islet cholesterol, including diet-induced obesity (9), *APOE* deficiency (6), *LXR* deficiency (36), *SCD1* deficiency (37), and *SREBP2* overexpression (38).

ABCA1-deficient β-cells showed a severely blunted exocytotic response in whole-cell capacitance measurements, even during prolonged membrane depolarization or during direct infusion of free Ca^{2+}, suggesting a functional defect downstream of Ca^{2+} entry into the β-cell. Because intracellular cholesterol depletion can very rapidly restore the exocytotic response, we propose that the action of ABCA1

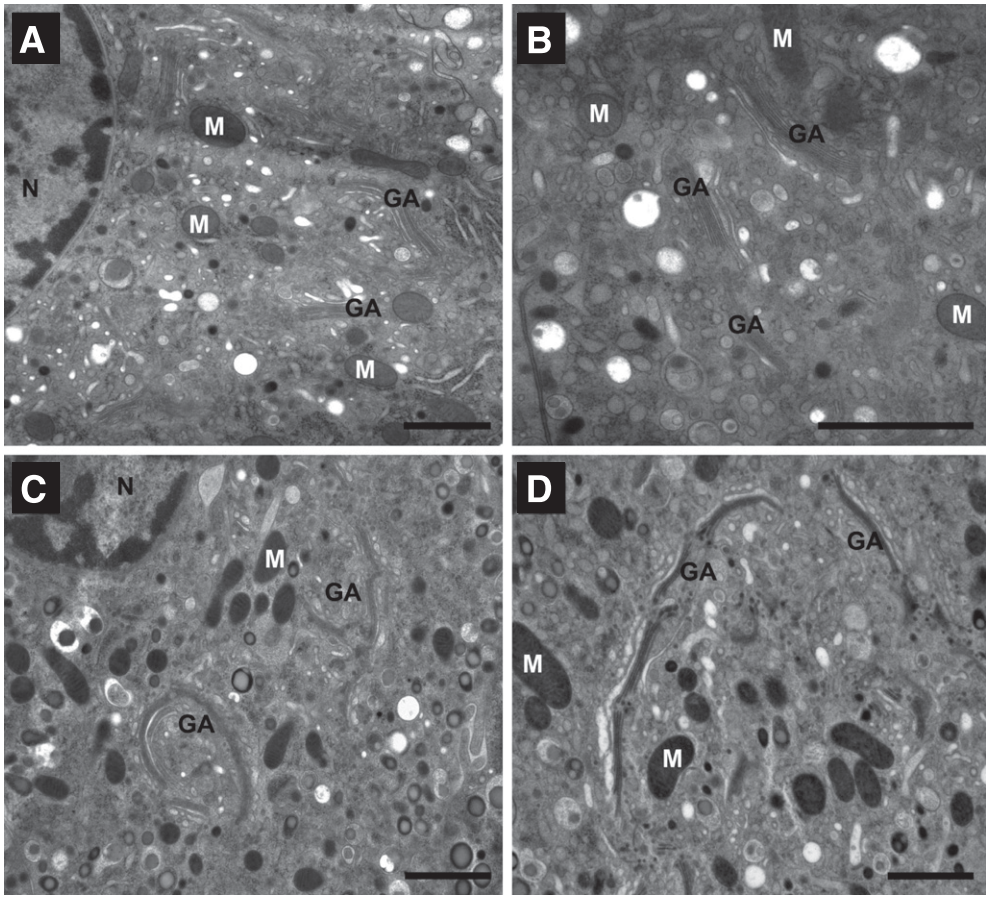

FIG. 5. Major alterations to Golgi organization in *ABCA1*$^{-P/-P}$ β-cells. The Golgi region in β-cells from control mice (*A* and *B*) reflected the hallmark architecture of Golgi membranes organized as a series of "compact regions" of stacked cisternae connected laterally to form a ribbon. Golgi region in β-cells from *ABCA1*$^{-P/-P}$ mice (*C* and *D*) demonstrated a tendency toward circular organization with more ordered and tightly stacked appearance, both at the level of increased cisternal stacking and increased lateral continuity along the length of the ribbon itself. GA, Golgi apparatus; M, mitochondrion; N, nucleus. Bars, 1 μm (except for inset, 500 nm).

is critical for maintaining local cholesterol homeostasis and the membrane environment required for correct membrane fusion events and insulin secretion.

An increasing body of literature suggests that cholesterol is critically involved in membrane fusion and exocytosis. As a membrane component, cholesterol can contribute to the fusion process by modulating the physical properties of the membrane, such as fluidity and curvature (39). In model membranes, cholesterol has been shown to stimulate membrane fusion by promoting hemifusion (40), regulating syntaxin clustering (41), and inducing conformational changes of VAMP-2 (42). In Ca^{2+}-triggered membrane fusion events, cholesterol contributes critical membrane curvature that lowers the energy barriers and promotes formation of fusion intermediates (43). Membrane cholesterol levels recently were shown to influence SNARE protein conformation patterns in neuroblastoma cells, affecting exocytosis (44) and indicating that regulation of membrane composition is essential for membrane fusion events and exocytosis. Lipid rafts have been implicated to play a role in insulin granule exocytosis in β-cells, because syntaxin-1, SNAP-25, VAMP-2, and the voltage-sensitive Ca^{2+} channel have been associated with cholesterol-enriched microdomains (22). We found that cholesterol loading increased the association of SNAP-25 with detergent-resistant membranes and that this was reversible by cholesterol depletion. In addition, we observed impaired signaling of the microdomain-sensitive EGF receptor pathway in β-cells lacking *ABCA1*. These findings suggest that in β-cells, there is altered microdomain organization during cholesterol accumulation and that normal ABCA1 activity may be critical for proper microdomain organization within membranes.

Whether loss of *ABCA1* affects microdomain organization only at the plasma membrane or also at the insulin granule membrane is currently unknown. Subcellular cholesterol distribution was recently reported to be important for insulin secretion in β-cells (45). Loss of the ABC transporter G1 (*ABCG1*), which mediates the transport of cholesterol toward HDL (46), resulted in decreased insulin secretion (45), although islet cholesterol levels were unaffected. Interestingly, cholesterol content of insulin granules was reduced. Administration of exogenous cholesterol restored insulin secretion in *ABCG1*-deficient cells. Together with our data, this suggests that precise regulation of cholesterol levels, both in the plasma membrane and in insulin granules, is crucial for insulin secretion.

In addition to a possible impairment in granule fusion events, several other factors may contribute to the reduction in insulin secretion present in *ABCA1*-deficient β-cells.

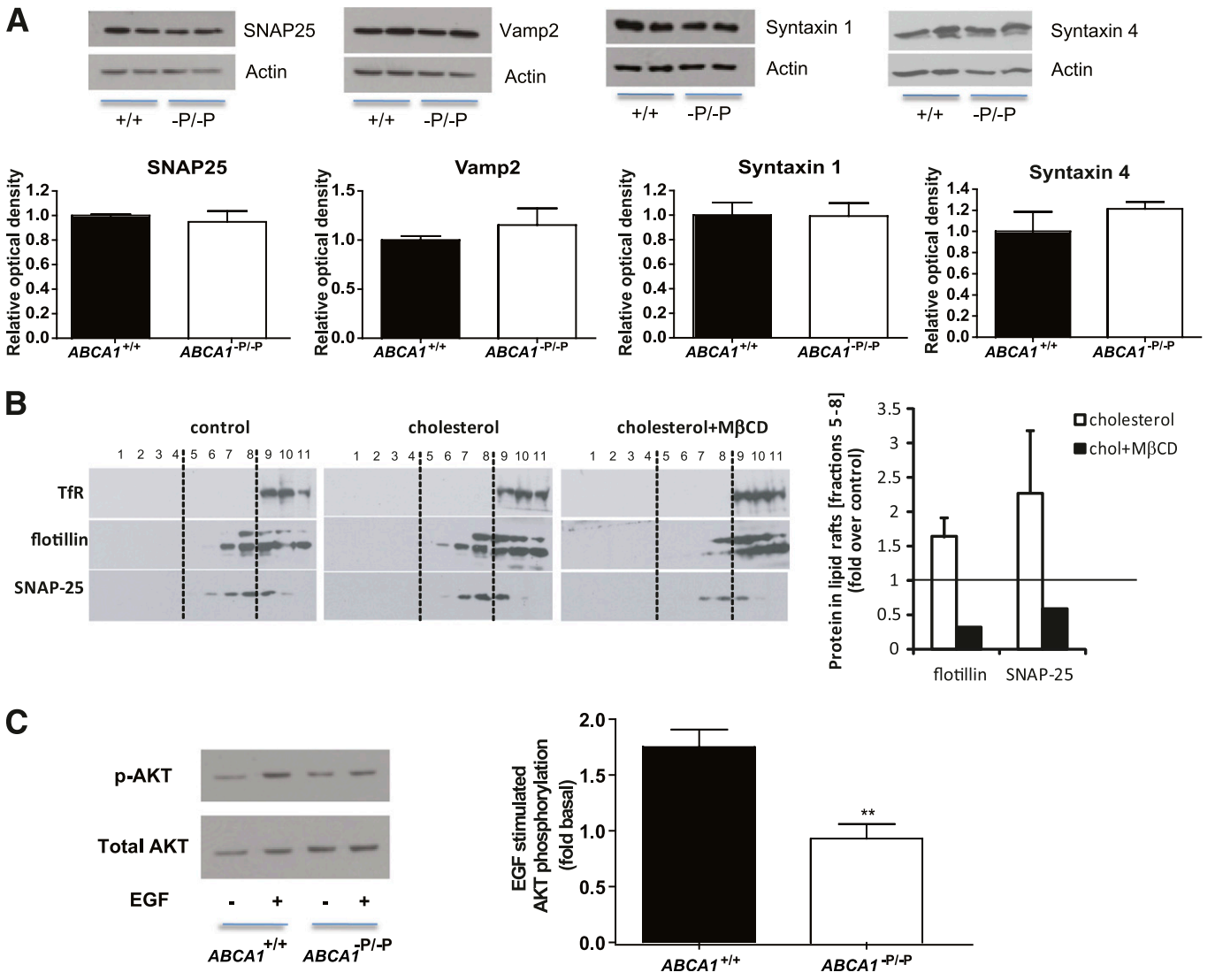

FIG. 6. Cholesterol accumulation alters membrane microdomain organization and impairs SNARE protein localization. *A*: SNAP-25, VAMP-2, syntaxin-1, and syntaxin-4 protein levels in isolated islets. Graphs represent pooled densitometric measurement of protein signal intensity from three separate experiments. Actin was used as the loading control. *B*: Representative Western blot of transferrin receptor (TfR), a marker for soluble fractions; flotillin, a marker for nonsoluble fractions; and SNAP-25 in lipid raft fractions of MIN6 cells treated with or without 2 mmol/L cholesterol (n = 2) for 30 min, followed by 10 mmol/L MβCD (n = 1) for an additional 30 min. Fractions 5–8 were designated as nonsoluble and band intensities quantified and expressed on the *right panel*. *C*: Representative Western blot of EGF-induced phosphorylation of AKT in isolated islets. Graphs represent pooled densitometric measurement of protein signal intensity from four separate experiments. **$P < 0.01$ compared with controls. (A high-quality color representation of this figure is available in the online issue.)

Calcium imaging revealed a small increase in basal $[Ca^{2+}]_i$ levels and a decrease in the depolarization-evoked $[Ca^{2+}]_i$ increase. Moderate elevations in basal $[Ca^{2+}]_i$ do not influence exocytosis (47), but this finding could indicate altered calcium homeostasis. Cholesterol loading of β-cells results in decreased calcium influx due to altered glucose metabolism (7,20). However, this seems not to be the mechanism responsible for the decreased glucose-evoked $[Ca^{2+}]_i$ increase in β-cells lacking *ABCA1*, because tolbutamide and KCl treatment also resulted in a decreased depolarization-evoked $[Ca^{2+}]_i$ increase. The observed changes in global Ca^{2+} signals in *ABCA1*-deficient β-cells may be related to differences in Ca^{2+}-induced Ca^{2+} release or to other processes downstream of the VDCCs, because we found no difference in VDCC activity compared with control cells.

In addition to functional changes, loss of β-cell *ABCA1* led to ultrastructural alterations in the Golgi apparatus and insulin granules. These changes may be attributable to altered cholesterol homeostasis. Cholesterol depletion affects Golgi organization and vesicle formation in enterocytes (48), and cholesterol loading of cultured cells results in Golgi vesiculation and inhibited exit from the *trans*-Golgi network (49). In addition, loss of *ABCA1* resulted in structural alterations in the Golgi network in enterocytes and in platelets (50). Loss of *ABCG1* leads to decreased insulin granule cholesterol levels and also affects insulin granule morphology, which is reversed after cholesterol loading (45). Although changed Golgi ultrastructure in *ABCA1*-deficient β-cells did not affect the number of docked insulin granules or total islet insulin levels (5), proinsulin processing was affected, as indicated by the increased plasma proinsulin levels in $ABCA1^{-P/-P}$ mice. In addition, the changed Golgi ultrastructure could affect membrane organization and thereby possibly the fusion competency of the insulin granules.

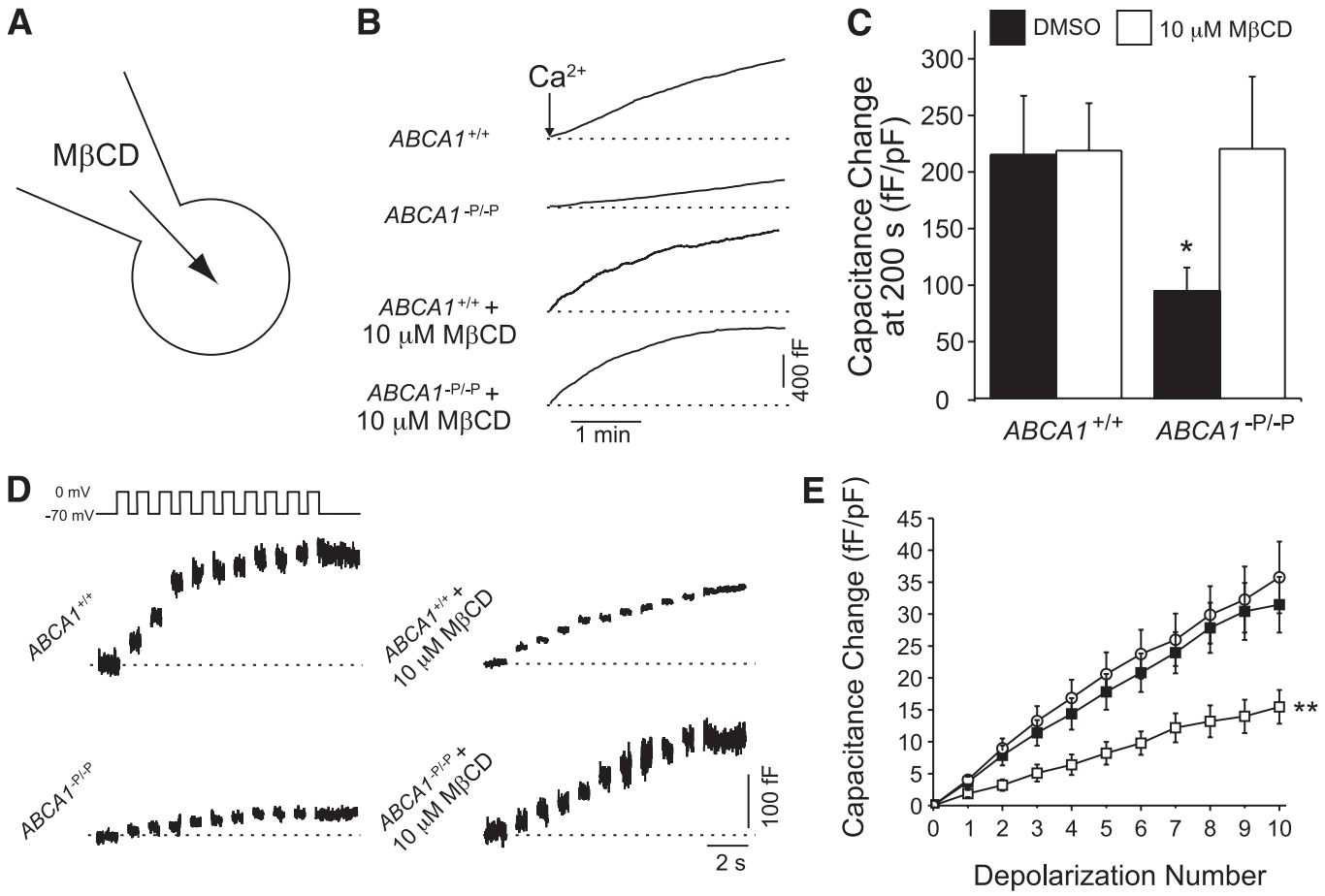

FIG. 7. The exocytotic defect in *ABCA1*$^{-P/-P}$ β-cells is rescued by acute intracellular cholesterol depletion. *A*: Whole-cell membrane capacitance from β-cells after intracellular dialysis with a low (10 μmol/L) concentration of MβCD to deplete cholesterol via the cell interior. *B*: Membrane capacitance during co-infusion of 200 nmol/L free–Ca^{2+} together with 10 μmol/L MβCD or an equal concentration of DMSO. *C*: The total capacitance increase, normalized to initial cell size, at 200 s after Ca^{2+} infusion (n = 13–16). *D*: The exocytotic response to a series of ten 500-ms depolarizations rescued in *ABCA1*$^{-P/-P}$ β-cells by intracellular cholesterol depletion. *E*: The cumulative capacitance response of *ABCA1*$^{+/+}$ (n = 21, ○) and *ABCA1*$^{-P/-P}$ β-cells dialyzed with DMSO (n = 23, □) or 10 μmol/L MβCD (n = 20, ■). For clarity, the *ABCA1*$^{+/+}$ + MβCD group is not shown, although this was not different from controls. *P < 0.05 and **P < 0.01 compared with controls.

Diabetes frequently coexists with abnormalities of plasma lipoproteins. Diabetic dyslipidemia is characterized by low levels of HDL and small dense LDL and by elevated triglycerides. Low levels of HDL are a risk factor for the development of diabetes (3), and HDL levels are inversely correlated with β-cell function in patients with type 2 diabetes (4), raising the question of whether low HDL may play a role in the pathogenesis of type 2 diabetes. ABCA1 regulates the rate-limiting step in HDL biogenesis and is critical in β-cell function and insulin secretion, suggesting that the low HDL level and impaired islet function observed in type 2 diabetes may share a common pathogenic mechanism. Lipid accumulation has been described in human islets, suggesting that cholesterol accumulation may occur in response to exposure to high levels of circulating lipids. Accumulation of cholesterol in islets was recently shown to differentiate between animals that become diabetic in response to high-fat feeding and those that do not (9), suggesting that islet cholesterol accumulation may be an important event in the pathogenesis of type 2 diabetes via the mechanisms we have described here. Together, these data suggest that ABCA1 and islet cholesterol levels may be an important mechanistic link between the low HDL level that frequently occurs in type 2 diabetes and the hallmark β-cell defect in this disorder.

In summary, our data suggest that impaired insulin secretion resulting from lack of *ABCA1* in β-cells may be attributed to defects at multiple levels: changes in membrane microdomain organization leading to redistribution of SNARE proteins, changes in $[Ca^{2+}]_i$ levels, and finally, changes in the Golgi ultrastructure leading to defects in insulin biosynthesis and processing, all of which may ultimately regulate vesicle fusion and insulin granule exocytosis. These data contribute to our understanding of the important role for cholesterol homeostasis in insulin secretion and glucose homeostasis.

ACKNOWLEDGMENTS

J.K.K. was supported by postdoctoral fellowship awards from the Canadian Institutes of Health Research (CIHR) and the Michael Smith Foundation for Health Research (MSFHR). N.W. was supported by a postdoctoral fellowship from the Heart and Stroke Foundation of Canada. X.-Q.D. was supported by a fellowship from the Alberta Heritage Foundation for Medical Research (AHFMR). The calcium

imaging was supported by a Canadian Diabetes Association Grant-in-Aid to J.D.J. The electron microscope work was supported by grants to B.J.M. from the Juvenile Diabetes Research Foundation International (2-2004-275). The Advanced Cryo-Electron Microscopy Laboratory housed at the Institute for Molecular Bioscience is a major node of the Australian Microscopy and Microanalysis Research Facility jointly supported by the Queensland state government's "Smart State Strategy" initiative. The exocytosis experiments were supported by a grant from CIHR to P.E.M., who holds the Canada Research Chair in Islet Biology and scholarships from AHFMR and the Canadian Diabetes Association. This work was supported by a CIHR grant to C.B.V., who is an MSFHR Senior Scholar. This work was supported by a CIHR grant to M.R.H., who holds a Canada Research Chair in Human Genetics and is a University of British Columbia Killam Professor.

No potential conflicts of interest relevant to this article were reported.

J.K.K. designed and performed the research and wrote the manuscript. N.W. performed the research, contributed to discussion, and reviewed and edited the manuscript. J.E.M.F. and X.-Q.D. performed the research. L.R.B. contributed to discussion and reviewed and edited the manuscript. G.J.S., G.P.M., A.J.C., R.T., and A.B. performed the research. J.D.J. and P.E.L. contributed to discussion and reviewed and edited the manuscript. B.J.M. performed the research, contributed to discussion, and reviewed and edited the manuscript. P.E.M. contributed to discussion and reviewed and edited the manuscript. C.B.V. designed the research, contributed to discussion, and reviewed and edited the manuscript. M.R.H. designed the research and wrote the manuscript.

The authors thank Dan S. Luciani, University of British Columbia, for advice regarding calcium imaging, and Terry D. Pape, Ting Yang, and Marc Wang, University of British Columbia, for technical assistance.

REFERENCES

1. Brunham LR, Kruit JK, Verchere CB, Hayden MR. Cholesterol in islet dysfunction and type 2 diabetes. J Clin Invest 2008;118:403–408
2. Adiels M, Olofsson SO, Taskinen MR, Borén J. Diabetic dyslipidaemia. Curr Opin Lipidol 2006;17:238–246
3. von Eckardstein A, Schulte H, Assmann G. Risk for diabetes mellitus in middle-aged Caucasian male participants of the PROCAM study: implications for the definition of impaired fasting glucose by the American Diabetes Association. Prospective Cardiovascular Münster. J Clin Endocrinol Metab 2000;85:3101–3108
4. Hermans MP, Ahn SA, Rousseau MF. log(TG)/HDL-C is related to both residual cardiometabolic risk and β-cell function loss in type 2 diabetes males. Cardiovasc Diabetol 2010;9:88
5. Brunham LR, Kruit JK, Pape TD, et al. Beta-cell ABCA1 influences insulin secretion, glucose homeostasis and response to thiazolidinedione treatment. Nat Med 2007;13:340–347
6. Kruit JK, Kremer PH, Dai L, et al. Cholesterol efflux via ATP-binding cassette transporter A1 (ABCA1) and cholesterol uptake via the LDL receptor influences cholesterol-induced impairment of beta cell function in mice. Diabetologia 2010;53:1110–1119
7. Hao M, Head WS, Gunawardana SC, Hasty AH, Piston DW. Direct effect of cholesterol on insulin secretion: a novel mechanism for pancreatic beta-cell dysfunction. Diabetes 2007;56:2328–2338
8. Cnop M, Hannaert JC, Grupping AY, Pipeleers DG. Low density lipoprotein can cause death of islet beta-cells by its cellular uptake and oxidative modification. Endocrinology 2002;143:3449–3453
9. Peyot ML, Pepin E, Lamontagne J, et al. Beta-cell failure in diet-induced obese mice stratified according to body weight gain: secretory dysfunction and altered islet lipid metabolism without steatosis or reduced beta-cell mass. Diabetes 2010;59:2178–2187
10. Drew BG, Duffy SJ, Formosa MF, et al. High-density lipoprotein modulates glucose metabolism in patients with type 2 diabetes mellitus. Circulation 2009;119:2103–2111
11. Vergeer M, Brunham LR, Koetsveld J, et al. Carriers of loss-of-function mutations in ABCA1 display pancreatic beta-cell dysfunction. Diabetes Care 2010;33:869–874
12. Brunham LR, Singaraja RR, Duong M, et al. Tissue-specific roles of ABCA1 influence susceptibility to atherosclerosis. Arterioscler Thromb Vasc Biol 2009;29:548–554
13. Wijesekara N, Dai FF, Hardy AB, et al. Beta cell-specific Znt8 deletion in mice causes marked defects in insulin processing, crystallisation and secretion. Diabetologia 2010;53:1656–1668
14. Johnson JD, Ahmed NT, Luciani DS, et al. Increased islet apoptosis in Pdx1+/- mice. J Clin Invest 2003;111:1147–1160
15. Dai XQ, Kolic J, Marchi P, Sipione S, Macdonald PE. SUMOylation regulates Kv2.1 and modulates pancreatic beta-cell excitability. J Cell Sci 2009;122:775–779
16. Pigeau GM, Kolic J, Ball BJ, et al. Insulin granule recruitment and exocytosis is dependent on p110gamma in insulinoma and human beta-cells. Diabetes 2009;58:2084–2092
17. Marsh BJ, Volkmann N, McIntosh JR, Howell KE. Direct continuities between cisternae at different levels of the Golgi complex in glucose-stimulated mouse islet beta cells. Proc Natl Acad Sci U S A 2004;101:5565–5570
18. Berglund ED, Li CY, Poffenberger G, et al. Glucose metabolism in vivo in four commonly used inbred mouse strains. Diabetes 2008;57:1790–1799
19. Rorsman P, Renström E. Insulin granule dynamics in pancreatic beta cells. Diabetologia 2003;46:1029–1045
20. Lee AK, Yeung-Yam-Wah V, Tse FW, Tse A. Cholesterol elevation impairs glucose-stimulated Ca2+ signaling in mouse pancreatic {beta}-cells. Endocrinology 2011;152:3351–3361
21. Barg S, Eliasson L, Renström E, Rorsman P. A subset of 50 secretory granules in close contact with L-type Ca2+ channels accounts for first-phase insulin secretion in mouse beta-cells. Diabetes 2002;51(Suppl. 1):S74–S82
22. Xia F, Gao X, Kwan E, et al. Disruption of pancreatic beta-cell lipid rafts modifies Kv2.1 channel gating and insulin exocytosis. J Biol Chem 2004;279:24685–24691
23. Takahashi N, Kishimoto T, Nemoto T, Kadowaki T, Kasai H. Fusion pore dynamics and insulin granule exocytosis in the pancreatic islet. Science 2002;297:1349–1352
24. Smukler SR, Tang L, Wheeler MB, Salapatek AM. Exogenous nitric oxide and endogenous glucose-stimulated beta-cell nitric oxide augment insulin release. Diabetes 2002;51:3450–3460
25. Kwan EP, Gaisano HY. Glucagon-like peptide 1 regulates sequential and compound exocytosis in pancreatic islet beta-cells. Diabetes 2005;54:2734–2743
26. MacDonald PE, Obermüller S, Vikman J, Galvanovskis J, Rorsman P, Eliasson L. Regulated exocytosis and kiss-and-run of synaptic-like microvesicles in INS-1 and primary rat beta-cells. Diabetes 2005;54:736–743
27. Ladinsky MS, Wu CC, McIntosh S, McIntosh JR, Howell KE. Structure of the Golgi and distribution of reporter molecules at 20 degrees C reveals the complexity of the exit compartments. Mol Biol Cell 2002;13:2810–2825
28. Eliasson L, Abdulkader F, Braun M, Galvanovskis J, Hoppa MB, Rorsman P. Novel aspects of the molecular mechanisms controlling insulin secretion. J Physiol 2008;586:3313–3324
29. Lang T. SNARE proteins and 'membrane rafts'. J Physiol 2007;585:693–698
30. Chamberlain LH, Burgoyne RD, Gould GW. SNARE proteins are highly enriched in lipid rafts in PC12 cells: implications for the spatial control of exocytosis. Proc Natl Acad Sci U S A 2001;98:5619–5624
31. Pike LJ, Casey L. Cholesterol levels modulate EGF receptor-mediated signaling by altering receptor function and trafficking. Biochemistry 2002;41:10315–10322
32. Zhuang L, Lin J, Lu ML, Solomon KR, Freeman MR. Cholesterol-rich lipid rafts mediate Akt-regulated survival in prostate cancer cells. Cancer Res 2002;62:2227–2231
33. Paila YD, Chattopadhyay A. Membrane cholesterol in the function and organization of G-protein coupled receptors. Subcell Biochem 2010;51:439–466
34. Navratil AM, Bliss SP, Roberson MS. Membrane rafts and GnRH receptor signaling. Brain Res 2010;1364:53–61
35. Chen YG. Endocytic regulation of TGF-beta signaling. Cell Res 2009;19:58–70
36. Gerin I, Dolinsky VW, Shackman JG, et al. LXRbeta is required for adipocyte growth, glucose homeostasis, and beta cell function. J Biol Chem 2005;280:23024–23031

37. Flowers JB, Rabaglia ME, Schueler KL, et al. Loss of stearoyl-CoA desaturase-1 improves insulin sensitivity in lean mice but worsens diabetes in leptin-deficient obese mice. Diabetes 2007;56:1228–1239
38. Ishikawa M, Iwasaki Y, Yatoh S, et al. Cholesterol accumulation and diabetes in pancreatic beta-cell-specific SREBP-2 transgenic mice: a new model for lipotoxicity. J Lipid Res 2008;49:2524–2534
39. Churchward MA, Coorssen JR. Cholesterol, regulated exocytosis and the physiological fusion machine. Biochem J 2009;423:1–14
40. Chang J, Kim SA, Lu X, Su Z, Kim SK, Shin YK. Fusion step-specific influence of cholesterol on SNARE-mediated membrane fusion. Biophys J 2009;96:1839–1846
41. Murray DH, Tamm LK. Clustering of syntaxin-1A in model membranes is modulated by phosphatidylinositol 4,5-bisphosphate and cholesterol. Biochemistry 2009;48:4617–4625
42. Tong J, Borbat PP, Freed JH, Shin YK. A scissors mechanism for stimulation of SNARE-mediated lipid mixing by cholesterol. Proc Natl Acad Sci U S A 2009;106:5141–5146
43. Churchward MA, Rogasevskaia T, Höfgen J, Bau J, Coorssen JR. Cholesterol facilitates the native mechanism of Ca2+-triggered membrane fusion. J Cell Sci 2005;118:4833–4848
44. Rickman C, Medine CN, Dun AR, et al. t-SNARE protein conformations patterned by the lipid microenvironment. J Biol Chem 2010;285:13535–13541
45. Sturek JM, Castle JD, Trace AP, et al. An intracellular role for ABCG1-mediated cholesterol transport in the regulated secretory pathway of mouse pancreatic beta cells. J Clin Invest 2010;120:2575–2589
46. Wang N, Lan D, Chen W, Matsuura F, Tall AR. ATP-binding cassette transporters G1 and G4 mediate cellular cholesterol efflux to high-density lipoproteins. Proc Natl Acad Sci U S A 2004;101:9774–9779
47. Barg S, Ma X, Eliasson L, et al. Fast exocytosis with few Ca(2+) channels in insulin-secreting mouse pancreatic B cells. Biophys J 2001;81:3308–3323
48. Hansen GH, Niels-Christiansen LL, Thorsen E, Immerdal L, Danielsen EM. Cholesterol depletion of enterocytes. Effect on the Golgi complex and apical membrane trafficking. J Biol Chem 2000;275:5136–5142
49. Ying M, Grimmer S, Iversen TG, Van Deurs B, Sandvig K. Cholesterol loading induces a block in the exit of VSVG from the TGN. Traffic 2003;4:772–784
50. Orsó E, Broccardo C, Kaminski WE, et al. Transport of lipids from Golgi to plasma membrane is defective in Tangier disease patients and Abc1-deficient mice. Nat Genet 2000;24:192–196